

Detection of Cyclotron Resonance Scattering Feature in High Mass X-ray Binary Pulsar SMC X-2

Gaurava K. Jaisawal* and Sachindra Naik†

Astronomy and Astrophysics Division, Physical Research Laboratory, Navrangapura, Ahmedabad - 380009, Gujarat, India

ABSTRACT

We report broadband spectral properties of the high mass X-ray binary pulsar SMC X-2 by using three simultaneous *NuSTAR* and *Swift*/XRT observations during its 2015 outburst. The pulsar was significantly bright, reaching a luminosity up to as high as $\sim 5.5 \times 10^{38}$ ergs s^{-1} in 1–70 keV range. Spin period of the pulsar was estimated to be 2.37 s. Pulse profiles were found to be strongly luminosity dependent. The 1–70 keV energy spectrum of the pulsar was well described with three different continuum models such as (i) negative and positive power-law with exponential cutoff, (ii) Fermi-Dirac cutoff power-law and (iii) cutoff power-law models. Apart from the presence of an iron line at ~ 6.4 keV, a model independent absorption like feature at ~ 27 keV was detected in the pulsar spectrum. This feature was identified as a cyclotron absorption line and detected for the first time in this pulsar. Corresponding magnetic field of the neutron star was estimated to be $\sim 2.3 \times 10^{12}$ G. The cyclotron line energy showed a marginal negative dependence on the luminosity. The cyclotron line parameters were found to be variable with pulse phase and interpreted as due to the effect of emission geometry or complicated structure of the pulsar magnetic field.

Key words: stars: neutron – pulsars: individual: SMC X-2 – X-rays: stars.

1 INTRODUCTION

Cyclotron absorption lines are the unique features observed in the spectrum of accretion powered X-ray pulsars with magnetic field of the order of $\sim 10^{12}$ G. These absorption like features are originated due to the resonant scattering between hard X-ray photons and electrons in quantized energy states (Mészáros 1992). These energy levels, known as Landau levels, are equi-spaced and depend on the strength of the magnetic field. The separation between Landau levels corresponds to the energy of the cyclotron resonance scattering feature and expressed by a relation $E_{cyc} = 11.6 B_{12} \times (1+z)^{-1}$ (keV), where B_{12} is the magnetic field in the unit of 10^{12} G and z is the gravitational red-shift. The detection of cyclotron absorption line is therefore an unique method to directly estimate the magnetic field of the accretion powered X-ray pulsars. Despite abundance of data from several previous X-ray missions, these features are only detected in ~ 25 accretion powered X-ray pulsars (Pottschmidt et al. 2012 and references therein).

SMC X-2 is one of the brightest transient X-ray pulsar in the Small Magellanic Cloud (SMC). It was discovered with *SAS-3* in 1977 at a luminosity of 8.4×10^{37} ergs s^{-1} in 2–11 keV energy band, assuming a distance of 65 kpc (Clark et al. 1978; Clark, Li & van Paradijs 1979). Since the discovery, the source was observed with

several observatories such as *HEAO*, *Einstein* and *ROSAT*, which established the transient nature of the pulsar (Marshall et al. 1979; Seward & Mitchell 1981; Kahabka & Pietsch 1996). Pulsation at ~ 2.37 s was discovered with the *RXTE* and *ASCA* observations during one of the major X-ray outburst observed in 2000 (Torii et al. 2000; Corbet et al. 2001; Yokogawa et al. 2001). The optical companion discovered by Crampton, Hutchings & Cowley (1978) was later resolved into two early spectral type stars (Schmidtke, Cowley & Udalski 2006). The I-band photometric studies of these stars with Optical Gravitational Lensing Experiment (OGLE) revealed that the northern star is the true optical companion of SMC X-2. This conclusion was derived based on the periodic variability observed in the magnitude (up to 1 mag) at a period of 18.62 ± 0.02 d (Schurch et al. 2011). A similar value of periodicity at 18.38 ± 0.02 d was obtained from the pulse-period evolution studies of the pulsar from *RXTE* observations (Townsend et al. 2011). Observed periodicity of ~ 18.4 d from two different approaches corresponds to orbital period of binary system. McBride et al. (2008) identified the optical companion as a O9.5 III–V emission star.

Since 2000, there was no report of any major X-ray activity (outburst) detected in the pulsar. Recently, an intense X-ray outburst was detected in 2015 September during which the pulsar luminosity reached up to as high as $\sim 10^{38}$ ergs s^{-1} (Negoro et al. 2015; Kennea et al. 2015). The pulsar spectra obtained from *XMM-Newton* and *Swift*/XRT observations during this outburst were described with cutoff power-law model with a soft blackbody compo-

* gaurava@prl.res.in

† snaik@prl.res.in

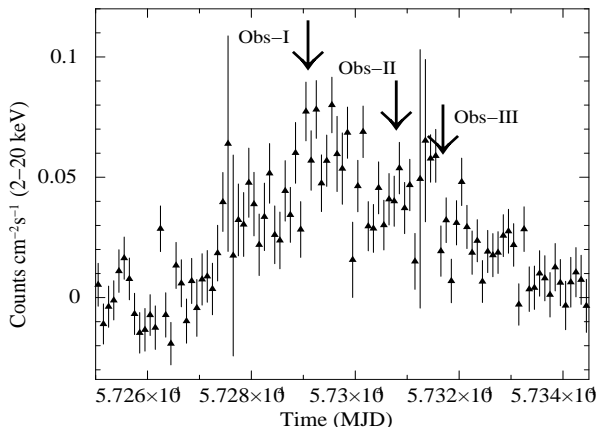


Figure 1. Light curve of the 2015 outburst of SMC X-2, observed with *MAXI* in 2–20 keV energy range covering the duration from 2015 August 16 (MJD 57250) to 2015 November 19 (MJD 57345), is shown. Arrows in the figure show the date of *NuSTAR* and *Swift*/XRT observations during the outburst.

ment at ~ 0.15 keV. In addition to a hard spectrum ($\Gamma \approx 0$), several emission lines from ionized N, O, Ne, Si and Fe were detected during this outburst (La Palombara et al. 2016). We have studied the 1–70 range energy spectrum of the pulsar by using the Nuclear Spectroscopy Telescope Array (*NuSTAR*) and *Swift*/XRT observations during the 2015 outburst. The details on observations, results and conclusions are presented in following sections of this letter.

2 OBSERVATION AND ANALYSIS

Following the report of X-ray outburst, Target of Opportunity (ToO) observations of SMC X-2 were performed with *NuSTAR* (Harrison et al. 2013) at three different epochs in 2015 September – October as shown in Fig. 1. Simultaneous *Swift*/XRT (Burrows et al. 2005) observations were also carried out at these epochs of the outburst. The details of the observations used in this paper are listed in Table 1. Hereafter, we used Obs-I (ObsIDs: 90102014002 & 00034073002), Obs-II (ObsIDs: 90102014004 & 00081771002) and Obs-III (ObsIDs: 90101017002 & 00034073042) to denote the first, second and third sets of *NuSTAR* and *Swift*/XRT data, respectively.

NuSTAR is the first hard X-ray focusing telescope sensitive in the 3–79 keV energy range. It consists of two independent grazing incident telescopes that focus the photons at two different focal planes, FPMA and FPMB. We have used standard NUSTAR-DAS software v1.4.1 of HEASoft version 6.16 to generate the barycentric corrected light curves, spectra, response matrices and effective area files. The source light curves and spectra were extracted from the FPMA and FPMB data by selecting a circular region around the source center. The radii of the circular regions used were 135, 100 and 100 arcsec for first, second and third *NuSTAR* observations, respectively. Background data products were accumulated in a similar manner by selecting circular regions of same size as quoted above and away from the source. We also used the *Swift*/XRT data for spectral analysis below 10 keV. We used the standard XRTPIPELINE for reprocessing the XRT data. The source and background spectra were extracted from the window timing mode event by considering the source and background regions in XSELECT package. The response file for XRT was generated by using the `xrtmkarf` tool.

Table 1. Log of simultaneous observations of SMC X-2 with *NuSTAR* and *Swift*/XRT.

Observatory/ Instrument	ObsID	Start Date (MJD)	Exposure (ks)
<i>NuSTAR</i>	90102014002	2015-09-25T21:51:08	24.5
<i>Swift</i> /XRT	00034073002	2015-09-25T22:32:58	1.8
<i>Swift</i> /XRT	00081771002	2015-10-12T21:30:58	1.5
<i>NuSTAR</i>	90102014004	2015-10-12T21:41:08	23
<i>Swift</i> /XRT	00034073042	2015-10-21T14:08:58	4
<i>NuSTAR</i>	90101017002	2015-10-21T21:31:08	26.7

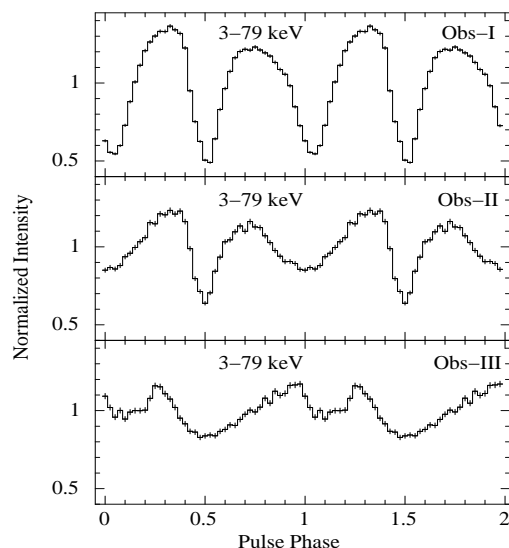


Figure 2. Pulse profiles of SMC X-2 obtained from the background subtracted light curves of FPMA detector of *NuSTAR* during first, second and third observations, respectively. Luminosity dependence of the pulse profiles can be clearly seen. The error bars in each panel represent 1σ uncertainties. Two pulses in each panel are shown for clarity.

3 RESULTS

Source and background light curves from *NuSTAR* data were extracted at 50 ms time resolution. We used the χ^2 -maximization method to estimate the barycentric corrected pulse period of the pulsar. The pulsation period at 2.37197(2), 2.37141(2) and 2.37257(2) s were detected in the X-ray light curves of the pulsar during Obs-I, Obs-II and Obs-III *NuSTAR* observations, respectively. The error in the pulse period was estimated for 1σ significance level. The pulse profiles in 3–79 keV range were generated by folding the background subtracted light curves at corresponding estimated spin periods from these observations and shown in Fig. 2. A strong luminosity dependence of the pulse profile can be clearly seen in the figure. During Obs-I (at the peak of the outburst), the pulse profile (top panel of Fig. 2) appeared double-peaked indicating the emissions or viewing of both the poles of the pulsar. However, significantly changed pulse profiles were observed during Obs-II & III (at the declining phase of the X-ray outburst) and are shown in second and third panels of the figure.

3.1 Pulse-phase-averaged spectroscopy

Spectral properties of SMC X-2 in broad energy range (1-70 keV) have been investigated for the first time and reported in this paper by using data from simultaneous observations with *NuSTAR* (3-70 keV range) and *Swift*/XRT (1-8 keV range). The procedure for spectral extraction was described in previous section. The source spectra were grouped to achieve >20 counts per channel bins. With appropriate background spectra, response matrices and effective area files, simultaneous spectral fitting in 1-70 keV range was carried out by using *Swift*/XRT and *NuSTAR* data for each of the three epochs of observations. *XSPEC* (ver. 12.8.2) package was used to do the spectral fitting. The spectral parameters were tied together during the fitting except the relative detector normalizations.

Standard continuum models such as high energy cutoff power-law (White et al. 1983), the Fermi-Dirac cutoff power-law (FDCut), the Negative and Positive power-law with Exponential cutoff (NPEX; Makishima et al. 1999) and cutoff power-law (CutoffPL) were used to fit the pulsar spectrum. We found that NPEX, FDCut and CutoffPL models can explain the pulsar continuum well for all three observations. However, an additional blackbody component was required to fit the source spectra obtained from Obs-II & Obs-III with CutoffPL model. An iron fluorescence emission line at ~ 6.4 keV was detected in the source spectrum. Apart from the iron emission line, an absorption-like feature at ~ 27 keV was also detected in the pulsar spectra obtained from all *NuSTAR* observations. This feature was detected in the source continuum in a model independent manner. We added a Gaussian absorption line (GABS) in the model to explain the absorption feature. The addition of GABS in the model improved the spectral fitting significantly yielding the reduced χ^2 close to 1. The residuals obtained from the spectral fitting with all three models are shown in Fig. 3 & 4 for Obs-I & II, respectively. A strong absorption like feature can be clearly visible in 20-30 keV energy range in second, third and fourth panels of the figures. This feature was found to be model independent and clearly detected in all three *NuSTAR* observations. We identified this feature as cyclotron absorption line of the pulsar. Best fitting parameters from the NPEX continuum model are given in Table 2 for all three observations. It can be seen that the cyclotron line energies during these observations are marginally different, showing a negative dependence on luminosity. The source flux was found to be relatively high during Obs-I compared to that during Obs-II & III. Although the cutoff energy is nearly same during these observations, the photon index is also showing a dependence on luminosity. A hard spectrum with photon index close to zero, i.e. almost flat spectrum, was observed during Obs-I.

3.2 Pulse-phase-resolved spectroscopy

Phase-resolved spectroscopy was performed to understand the variation of the parameters of cyclotron resonance scattering features with the pulse phase of the pulsar. As the pulsar was relatively bright during the first observation, we accumulated the phase-resolved spectra in 8 pulse-phase bins from the first *NuSTAR* observation. Using corresponding background, response and effective area files, the phase-resolved spectroscopy was carried out in the 3-70 keV energy range. The NPEX continuum model was used to fit the phase-resolved spectra. The absorption-like feature, as seen in phase-averaged spectra, was also clearly detected in each of the phase-resolved spectra. A GABS component was included in the continuum model for the cyclotron absorption line. While fitting, the equivalent hydrogen column density (N_H), iron line parameters

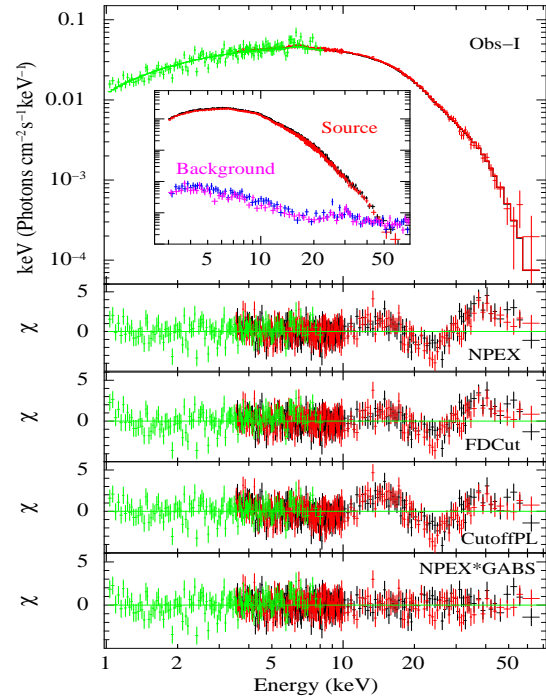


Figure 3. The energy spectrum of SMC X-2 in 1-70 keV range obtained from FPMA and FPMB detectors of *NuSTAR* and *Swift*/XRT data during the first observation along with the best-fit model comprising a NPEX continuum model with an iron emission line and a Gaussian absorption component for cyclotron resonance scattering feature. The second, third and fourth panels show the contributions of the residuals to χ^2 when pulsar continuum was fitted with NPEX, FDCut and CutoffPL models, respectively. In all these panels, an absorption like feature in 20-30 keV range is clearly visible. The fifth panel shows the residuals for NPEX model after including a GABS component for cyclotron line. The background subtracted source spectra and background spectra are shown in the inset. It can be seen that the background is relatively much lower than the source counts during the observation.

and cyclotron width were fixed to corresponding phase-averaged values as given in Table 2.

The cyclotron line parameters such as line energy and strength obtained from the phase-resolved spectroscopy are shown in Fig. 5. Both the parameters are marginally variable with pulse-phases of the pulsar. The energy of cyclotron line was found to be variable between 23 to 28 keV (<20% of phase-averaged value) with maximum at around 0.5 pulse phase. The strength of cyclotron line was found to be varying between 4 to 8 and following similar pattern to that of cyclotron line energy. The errors in the figure are estimated for 90% confidence level. We also checked the variation of cyclotron line energy with pulse phase by fixing the line strength at the phase-averaged value and vice versa. However, there was no notable change in the pulse phase dependence of these parameters apart from a marginal improvement in the estimated errors at each of the pulse phase values.

4 DISCUSSION AND CONCLUSIONS

As the magnetic field of accretion powered binary X-ray pulsars is in the order of 10^{12} G, the cyclotron resonance scattering features are expected to be detected in hard X-ray (10–100 keV) ranges. Therefore, the possibility of detection of such features in the hard

Table 2. Best-fitting parameters (with 90% errors) obtained from the spectral fitting of three *NuSTAR* and *Swift*/XRT observations of SMC X-2 during 2015 outburst with the NPEX continuum model with an iron emission line and cyclotron absorption line.

Parameter	Obs-I		Obs-II		Obs-III	
	NPEX	NPEX×GABS	NPEX	NPEX×GABS	NPEX	NPEX×GABS
N_H^a	$0.1^{+0.03}_{-0.1}$	0.18 ± 0.06	0.7 ± 0.1	0.5 ± 0.1	0.8 ± 0.1	0.6 ± 0.1
Photon index	-0.1 ± 0.02	0.04 ± 0.04	0.78 ± 0.05	0.62 ± 0.08	1.05 ± 0.09	0.81 ± 0.09
E_{cut} (keV)	4.4 ± 0.1	4.8 ± 0.1	4 ± 0.1	4.6 ± 0.2	4 ± 0.1	4.5 ± 0.2
Fe line energy (keV)	6.42 ± 0.08	6.42 ± 0.08	6.32 ± 0.09	6.35 ± 0.08	6.31 ± 0.15	6.34 ± 0.1
Fe line eq. width (eV)	47 ± 10	72 ± 14	88 ± 18	83 ± 18	70 ± 20	70 ± 20
Cycl. line energy (E_c) (keV)	–	27.2 ± 0.9	–	29 ± 1.6	–	$29.8^{+2.7}_{-1.7}$
Cycl. line width (σ_c) (keV)	–	6.4 ± 1.0	–	7 ± 1.5	–	$7.2^{+2.3}_{-1.4}$
Cycl. line strength (τ_c)	–	6 ± 2	–	9^{+5}_{-3}	–	9^{+9}_{-4}
Luminosity ^b (1-70 keV)	–	5.5 ± 0.5	–	2.7 ± 0.3	–	1.8 ± 0.2
Reduced- χ^2 (dofs)	1.55 (582)	1.04 (579)	1.29 (551)	1.02 (548)	1.27 (596)	1.08 (593)

^a : Equivalent hydrogen column density (in 10^{22} atoms cm^{-2}); ^b : Luminosity in 10^{38} ergs s^{-1} , assuming a distance of 61 kpc (Hilditch, Howarth & Harries 2005).

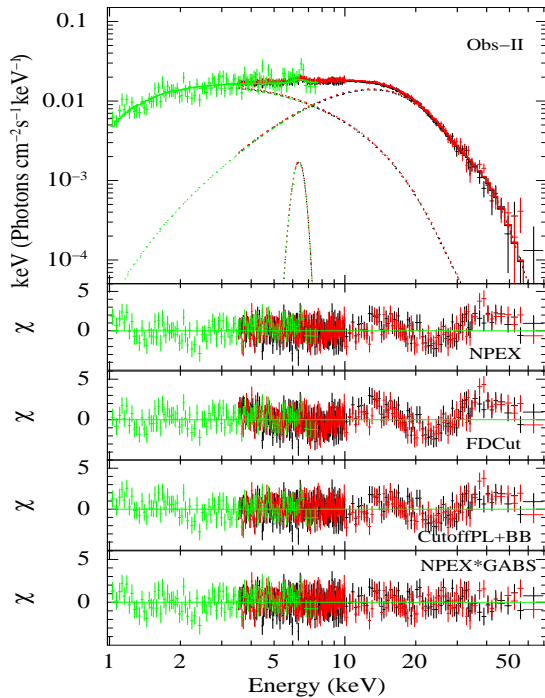


Figure 4. The energy spectrum of SMC X-2 in 1-70 keV range obtained from FPMA and FPMB detectors of *NuSTAR* and *Swift*/XRT data during second observation along with the best-fit model comprising a NPEX model with an iron emission line and a Gaussian absorption component for a cyclotron line. The second, third and fourth panels show the contributions of the residuals to χ^2 when the continuum was fitted with NPEX, FDCut and CutoffPL (with blackbody) models, respectively. In all these panels, an absorption like feature in 20-30 keV range is clearly visible. The fifth panel shows the residuals for NPEX model after including a GABS component for cyclotron line.

X-ray spectrum becomes high when the source is very bright. During the 2015 giant X-ray outburst, the luminosity of SMC X-2 was estimated to be significantly high ($\sim 5.5 \times 10^{38}$ ergs s^{-1}) compared to earlier reported values. This high luminosity phase of SMC X-2 enabled us to detect the presence of cyclotron resonance scattering feature at ~ 27 keV for the first time in the pulsar spectrum which

has not been reported earlier. As mentioned earlier, the cyclotron resonance scattering features are directly related to the magnetic field strength of the pulsar. Corresponding to the detected cyclotron line energy of ~ 27 keV, the magnetic field of SMC X-2 was estimated to be $\sim 2.3 \times 10^{12}$ G. Although the cyclotron lines are rarely detected in the broad-band spectrum of accretion powered binary X-ray pulsars, the hard X-ray focusing capability of *NuSTAR* remarkably contributed in the discovery of cyclotron lines in new sources. This helped in increase of the number of cyclotron sources to about 25.

During *NuSTAR* observations, the luminosity of the pulsar was very high ($> 10^{38}$ ergs s^{-1}). It is possible that SMC X-2 was accreting in the super-critical accretion regime during 2015 X-ray outburst. At such high luminosity state, a radiation-dominated shock can be formed above the neutron star surface which decelerates in-falling matter before settling on to the surface (Becker et al. 2007). Cyclotron lines are expected to be formed close to the shock region. As the luminosity increases, the shock region shifted upwards in the accretion column where relatively low value of cyclotron line energy is observed. This results a negative dependence between cyclotron line energy and luminosity. We observed the expected negative correlation during *NuSTAR* observations of SMC X-2. This can be explained in terms of changes in shock height or line forming region with luminosity. Only two X-ray pulsars such as 4U 0115+63 (Nakajima et al. 2006) and V 0332+53 (Tsygankov et al. 2010) are known showing such negative correlation.

For the first time, we presented a detailed phase-resolved spectroscopy of cyclotron parameters for SMC X-2. The cyclotron line energy and its strength were found to be marginally variable with pulse-phase of the pulsar. Numerical simulations based on cyclotron line features suggest that the 10-20% variation in the cyclotron line parameters can be attributed to the viewing angle of the emission geometry. However, $> 30\%$ variation in parameters can be expected from distortion in magnetic dipole geometry of the pulsar (Schönherr et al. 2007; Mukherjee & Bhattacharya 2012). During *NuSTAR* observations, the cyclotron line energy was variable within 20% of the phase-averaged value which can be explained as the effect of viewing angle or local distortion in the magnetic field, as seen in other X-ray binary pulsars such as Cep X-4 (Jaisawal & Naik 2015) and GX 304-1 (Jaisawal et al. 2016).

In summary, we report the discovery of cyclotron absorption

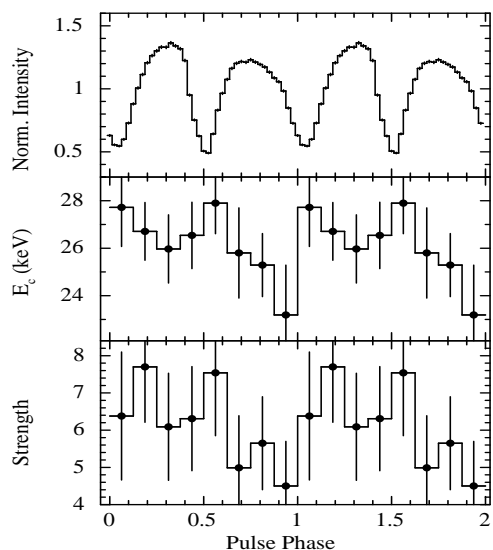


Figure 5. Spectral parameters (with 90% errors) obtained from the phase-resolved spectroscopy of SMC X-2 during first *NuSTAR* observation. Top panel shows the pulse profile in the 3-79 keV energy range. The values of cyclotron line parameter such as energy E_c and strength τ are shown in second and third panels, respectively.

line at ~ 27 keV in SMC X-2 with *NuSTAR* and *Swift*/XRT observations at three epochs during 2015 X-ray outburst. The cyclotron line was detected in all three observations in a model independent manner. Using the detected cyclotron line parameters, the magnetic field of the pulsar was estimated to be $\sim 2.3 \times 10^{12}$ G. A negative dependence between cyclotron line energy and luminosity in SMC X-2 can be explained as due to the change in the shock height or line forming region with luminosity. The phase-resolved spectroscopy from first *NuSTAR* observation also revealed the presence of cyclotron line at different phases. The pulse-phase variation of the cyclotron parameters can be attributed as the effect of viewing angle or role of complicated magnetic field of the pulsar.

ACKNOWLEDGMENTS

We sincerely thank the referee for his/her valuable comments and suggestions which improved the paper. The research work at Physical Research Laboratory is funded by the Department of Space, Government of India. The authors would like to thank all the *NuSTAR* and *Swift* team members for ToO observations. This research has made use of data from HEASARC Online Service, and the *NuSTAR* Data Analysis Software (*NuSTARDAS*) jointly developed by the ASI Science Data Center (ASDC, Italy) and the California Institute of Technology (USA).

REFERENCES

Becker P. A., Klochov D., Schönherr G., et al. 2012, *A&A*, 544, A123
 Burrows D. N., Hill J. E., Nousek J. A., et al. 2005, *SSRv*, 120, 165
 Clark G., Doxsey R., Li F., Jernigan J. G., van Paradijs J., 1978, *ApJ*, 221, L37
 Clark G., Li F., van Paradijs J., 1979, *ApJ*, 227, 54
 Corbet R. H. D., Marshall F. E., Coe M. J., Laycock S., Handler G., 2001, *ApJ*, 548, L41
 Crampton D., Hutchings J. B., Cowley A. P., 1978, *ApJ*, 223, L79
 Harrison F. A., Craig W. W., Christensen F. E., et al. 2013, *ApJ*, 770, 103

Hilditch R. W., Howarth I. D., Harries T. J., 2005, *MNRAS*, 357, 304
 Jaisawal G. K., Naik S., 2015, *MNRAS*, 453, L21
 Jaisawal G. K., Naik S., Epili P., 2016, *MNRAS*, 457, 2749
 Kahabka P., Pietsch W., 1996, *A&A*, 312, 919
 Kennea J. A. et al., 2015, *Astron. Telegram*, 8091, 1
 La Palombara N., Sidoli L., Pintore F., Esposito P., Mereghetti S., Tiengo A., 2016, *MNRAS*, 458, L74
 Makishima K., Mihara T., Nagase F., Tanaka Y., 1999, *ApJ*, 525, 978
 Marshall F. E., Boldt E. A., Holt S. S., Mushotzky R. F., Pravdo, S. H., Rothchild R. E., Serlemitsos P. J., 1979, *ApJS*, 40, 657
 McBride V. A., Coe M. J., Negueruela I., Schurch M. P. E., McGowan K. E., 2008, *MNRAS*, 388, 1198
 Mészáros P., 1992, High-energy radiation from magnetized neutron stars
 Mukherjee D., Bhattacharya D., 2012, *MNRAS*, 420, 720
 Nakajima M., Mihara T., Makishima K., Niko H., 2006, *ApJ*, 646, 1125
 Negoro H. et al., 2015, *Astron. Telegram*, 8088, 1
 Pottschmidt K. et al., 2012, in Petre R., Mitsuda K., Angelini L., eds, *AIP Conf. Proc. Vol. 1427, Suzaku 2011: Exploring the X-ray Universe: Suzaku and Beyond*. Am. Astron. Soc., Melville, NY, p. 60
 Schmidtke P. C., Cowley A. P., Udalski A., 2006, *AJ*, 132, 971
 Schönherr G., et al. 2007, *A&A*, 472, 353
 Schurch M. P. E., Coe M. J., McBride V. A., Townsend L. J., Udalski A., Haberl F., Corbet R. H. D., 2011, *MNRAS*, 412, 391
 Seward F. D., Mitchell M. 1981, *ApJ*, 243, 736
 Torii K., Kohmura T., Yokogawa J., Koyama K., 2000, *IAU Circ.*, 7441, 2
 Townsend L. J., Coe M. J., Corbet R. H. D., Hill A. B., 2011, *MNRAS*, 416, 1556
 Tsygankov S. S., Lutovinov A. A., & Serber A. V., 2010, *MNRAS*, 401, 1628
 Yokogawa J., Torii K., Kohmura T., Koyama K., 2001, *PASJ*, 53, 227
 White N. E., Swank J. H. & Holt S. S., 1983, *ApJ*, 270, 711